The Scattering of Neutrons of Energy between 12.0 Mev and 13.0 Mev by Protons

J. S. LAUGHLIN AND P. G. KRUGER
Department of Physics, University of Illinois, Urbana, Illinois
(Received September 25, 1947)

The angular distribution of the recoil protons projected during the scattering of neutrons by protons has been investigated in a methane-filled, high pressure cloud chamber. A deuterium gas target bombarded with 10 Mev deuterons provided the high energy neutron source. The spectrum of the neutrons from this source, which entered the cloud chamber through a collimator, was surveyed and showed a group of high energy neutrons superimposed on a continuous background. Examination of the data with rigorous selection criteria to determine those recoils projected by the scattering of neutrons between 12.0 Mev and 13.0 Mev yielded a total of 1573 recoil protons. The azimuthal and recoil angle distributions of these protons have been analyzed. A ratio of the differential cross sections for neutron scattering in the backward direction to scattering in a direction perpendicular to that of the incident neutron beam, of unity (spherically symmetric scattering) or slightly greater than unity can be consistent with these data.

THEORETICAL predictions concerning the angular distribution to be expected in the scattering of high energy neutrons by protons vary widely, depending on the nature of the forces assumed for the neutron-proton interaction. Because of the fundamental importance of obtaining a more accurate knowledge of the nature of the neutron-proton interaction, this study of the angular distribution of recoil protons from the scattering of high energy neutrons has been made. Several other authors[1-3] have also mentioned the desirability of obtaining further data on the scattering of high energy neutrons by protons.

In this report the experimental study of the scattering of neutrons between 12.0 Mev and 13.0 Mev in energy is described. The angular distribution was studied in a methane-filled, high pressure (25 atmospheres) cloud chamber. The University of Illinois cyclotron was used to bombard deuterium gas with 10 Mev deuterons for the neutron source.

Previous experiments[4-6] indicated that at lower energies (2.6 Mev) the neutron-proton scattering process is spherically symmetric. However, the results of other experimenters at high energies (12.5 Mev to 14.0 Mev) have indicated large deviations from spherically symmetric scattering. Amaldi and his collaborators[7] reported a determination of the ratio of the differential cross sections for scattering of 12.5 Mev neutrons in the backward direction to the scattering in a perpendicular direction with respect to the incident neutron beam in the center-of-mass system of 0.71 ± 0.04 and a ratio of 0.53 ± 0.03 for neutrons with an average energy of 13.3 Mev. They employed proportional counters in triple coincidence to detect the recoil protons. Champion and Powell[8] employed photographic emulsions as detectors to study the same problem. Their results with neutrons of about 13.0 Mev energy were first reported to be in general agreement with those of Amaldi. Later results by Powell[9] indicate spherically symmetric scattering in the center-of-mass system.

The high pressure cloud chamber was used in this experimental study of the angular distribution of the neutron-proton scattering process. The chamber body was constructed by the Westinghouse Electric and Manufacturing Com-

[1] William Rarita, Julian Schwinger, and H. A. Nye, Phys. Rev. 59, 209 (1941).
[2] Lamek Hulthén, Phys. Rev. 63, 383 (1943).
[3] W. Pauli, *Meson Theory of Nuclear Forces* (Interscience Publishers, Inc., New York, 1946) p. 56.
[4] P. G. Kruger, W. E. Shoupp, and F. W. Stallman, Phys. Rev. 52, 678 (1937).
[5] T. W. Bonner, Phys. Rev. 52, 685 (1937).
[6] P. I. Dee and C. W. Gilbert, Proc. Roy. Soc. 163, 265 (1937).
[7] E. Amaldi, D. Bocciarelli, B. Ferretti, and G. C. Trabacchi, Naturwiss. 30, 582 (1942).
[8] F. C. Champion and C. F. Powell, Proc. Roy. Soc. A183, 64 (1944).
[9] G. Wentzel, Rev. Mod. Phys. 19, 10 (1947); (see footnote 38).

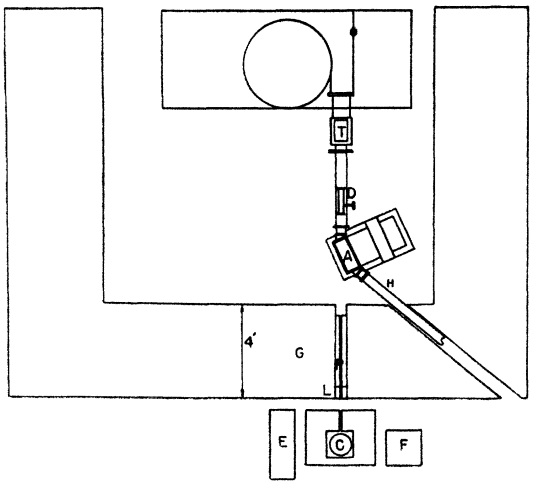

FIG. 1. Experimental arrangement. T indicates location of copper target containing a hole, D the deuterium target, A the analyzer magnet, P the paraffin collimator, L the lead collimator, C the high pressure cloud chamber, E the air compressor, F the control panel, G the shielding tanks around the cyclotron, and H the exit tube.

pany,[10] and was modified and the system completed at the University of Illinois. The cloud chamber interior has an inside diameter of $5\frac{3}{4}$ inches and a height of 3 inches. Expansion is caused by reducing the pressure underneath the piston. The cloud chamber operation was controlled by a cam system which, in conjunction with time delay relays, permitted sensitive and independent adjustment of the cycle time and of the time intervals between operation of the various components of the cloud chamber system. Illumination was provided by a mercury capillary arc. A reflector and double lens system concentrated the light for illuminating the cloud chamber in a parallel well-defined beam. A sweep-field voltage of about 2000 volts was applied between expansions. The cycle time was varied between two and three minutes, depending on equilibrium conditions in the chamber. The camera used was so designed that the film was accurately positioned and this position exactly reproducible. The camera used 35 mm film and contains an $f/2$ Ektar lens of 45 mm focal length. Each photograph contained three views of the chamber, a central view and two reflected views from two parallel mirrors perpendicular to the light beam and mounted rigidly in the mirror box which supported the camera above the chamber.

The vapor for track formation was provided by 10 cc of a 60 percent solution of isopropyl alcohol in distilled water. After evacuation, the chamber was filled with 99 percent pure methane gas to a gauge pressure of 335 pounds per square inch. The impurity in the methane consisted of higher order hydrocarbons.

The incident neutrons were detected by observing recoil protons projected from elastic collisions. The energy of the incident neutron E_n and the proton recoil E_p are related by the expression $E_p = E_n \cos^2\phi$, where ϕ is the recoil angle of the proton relative to the direction of the incident neutron in the laboratory system.

Three quantities were measured for each proton track, the recoil angle ϕ, the azimuthal angle θ, and its length L. The angle between the vertical direction and the projection of the proton track in a plane normal to the incident neutron beam is the azimuthal angle for that track. To measure these quantities, the tracks were reprojected through the same optical system in which they were photographed. Upon reprojection, the film was accurately positioned in the camera and illuminated by an arc. The three stereoscopic views of each track were projected on a ground glass screen. This screen, mounted on two rigid side arms attached to the stereoscopic mirror system, allowed one degree of rotational freedom and one degree of translational freedom. The viewing screen was adjusted until the stereoscopic images of a given proton track coincided and were in focus. A measuring engine was then used to measure the ϕ, θ, and L. This engine contained a lucite ruler graduated in millimeters. Adjustment of two bearings allowed this ruler to assume any direction and coincide with any proton track focused on the screen. Each of these bearings contained a pointer and an associated scale graduated in degrees. One of these indicated the recoil angle ϕ, while the other indicated the azimuthal angle θ. Thus ϕ, θ, and L could be simultaneously recorded. The length of each track was read to the nearest millimeter and the lengths were reproducible to one millimeter. The angles were read to the nearest degree. The recoil angle readings were reproducible after removing the film, replacing it and

[10] The cloud chamber was made available to the University of Illinois through Dr. W. E. Shoupp of the Westinghouse Electric and Manufacturing Company Research Laboratory.

readjusting for coincidence of the stereoscopic images, to within $\pm 2°$ and the azimuthal angles to within $\pm 4°$.

The direction of the incident neutrons was well known, since the neutrons were collimated by passing through a hole one-half inch in diameter through the water tanks surrounding the cyclotron. The collimation consisted of a tubular paraffin plug three feet long, with an outside diameter of six inches and an inside diameter of one-half inch. This paraffin plug, together with a lead plug six inches long with the same diameters, was placed in a cylindrical pipe through the water tanks. The cloud chamber was shielded from gamma-rays by lead blocks eleven inches thick placed around the chamber. A $\frac{5}{8}$-inch hole was bored through these blocks in a straight line with the collimator hole through the water tanks surrounding the cyclotron. The water in these tanks was saturated with boron, which aided in reducing to a negligible amount the number of neutrons which escaped through the tanks surrounding the cyclotron. The cloud chamber was so aligned with respect to the collimator that the neutrons passed through the center of the chamber along a diameter. In the photographs, over 95 percent of all proton tracks started in the central one-half inch diameter cylinder. Considering the relative volume of this cylinder to the illuminated volume of the chamber, less than one-half of one percent of the tracks originating in the central cylinder could have been due to stray neutrons. The collimation was thus successful in localizing the direction and path of the neutrons through the chamber.

A prolific source of high energy neutrons was necessary to make the cloud chamber method of studying the angular distribution possible. The neutrons from various targets bombarded by 10 Mev deuterons were investigated in a position at right angles to the incident deuteron beam before a satisfactory source was finally achieved in the forward direction. With the collimator and cloud chamber in the position at right angles to the deuteron beam, thin and thick targets of lithium, copper, beryllium, and aluminum were bombarded and the neutron energies and proton recoil intensities observed.[11] None of these targets gave a sufficient number of high energy neutrons to make a cloud chamber examination of the scattering problem feasible.

The d,d reaction is known to give a single monoenergetic group of neutrons when bombarded with monoenergetic deuterons:

$$_1D^2 + {}_1D^2 = {}_2\mathrm{He}^3 + {}_0n^1 + 3.26 \text{ Mev}.$$

The highest energy neutrons are ejected in the forward direction from the target, so the high pressure cloud chamber was stationed in front of the forward porthole of the water tanks. Figure 1 shows the general experimental arrangement. The deuteron beam passed through a one-inch hole in a copper target at T. After passing through the deuterium target at D, the deuteron beam was deflected by the analyser magnetic field at A and passed part way down the exit tube H. This prevented neutrons from sources other than the target entering the cloud chamber. The current in the analyzer magnet coils was increased somewhat above the value which would send the beam completely through the exit tube outside the tanks, so that it terminated on the exit tube well inside the water tank. The combined effect of the water and boron in these tanks made negligible the number of neutrons of energy above a few Mev passing through the tanks. The deuterium gas target holder is shown in Fig. 2. The end foils were one and one-half mil Duralumin foil. The stopping power of the deuterium gas for a 10 Mev deu-

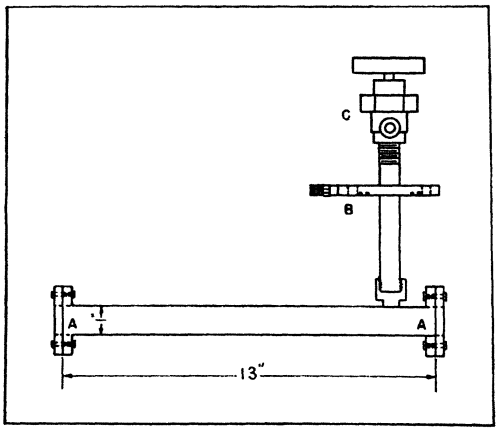

FIG. 2. Deuterium gas target. Location of the Duralumin windows is indicated by A, B indicates the flange which made a vacuum seal to the entrance tube, and C indicates the valve.

[11] J. S. Laughlin and P. G. Kruger, Phys. Rev. 71, 484 (1947).

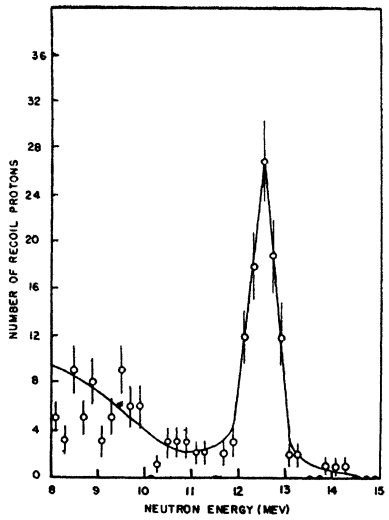

FIG. 3. Spectrum of recoil protons projected by neutrons from the deuterium gas target bombarded with 10 Mev deuterons.

teron was 0.52 Mev. Duralumin foils were chosen for the target windows, since they made it possible to use thicknesses with sufficiently high tensile strength to withstand atmospheric pressure which still had a low stopping power, and since both the aluminum and copper neutron spectrum observed in the right angle position had very low relative intensities for high energy neutrons above 9 Mev. Duralumin consist of about 94 percent aluminum, 4.2 percent copper, 0.7 percent manganese, 0.5 percent magnesium, 0.2 percent silicon, and 0.4 percent iron. The target could be evacuated and filled with gas without disturbing the vacuum of the cyclotron chamber.

0.85 Mev was the calculated maximum spread in the energy of the neutrons produced in this target resulting from inhomogeneity in energy of the incident deuterons, straggling in the foils, variation of magnetic field in the cyclotron during operation, and thickness of target. The median absolute energy was calculated to be 12.5 ± 0.2 Mev. The intensity of this group relative to the continuous background could not be predicted.

The cloud chamber was used to survey the high energy neutron spectrum of this target; collimation arrangement and about 900 photographs were taken for this purpose. The cyclotron deuterium arc was struck 0.05 sec. after each expansion had started. This insured that the chamber was about three-fourths expanded before irradiation.

In the calculation of the neutron energies, a single value of the stopping power was employed, since the spectrum was being examined over only the high energy range where the stopping power of methane has very small dependence on the proton energy. At a gauge pressure of 301.5 pounds per square inch, the stopping power of the chamber was 17.9 and each measured track length was multiplied by this amount. A range-energy curve constructed from a table published by Pollard and Davidson[12] was used to convert these lengths into proton energies. The relation $E_n=E_p/\cos^2\phi$ was then used to obtain the energies of the incident neutrons. Those tracks which were distinct, fully illuminated, entirely in the chamber, and which originated in the neutron beam along a diameter of the chamber were suitable for data. Although all tracks with scattering angles up through 50° were measured, only those at angles equal to or less than 40° were used in the calculations for the spectral survey. A total of 161 of the measured tracks corresponded to a neutron energy greater than 8 Mev. Figure 3 shows the results plotted in number of recoil protons versus neutron energy. A definite group of fairly energetically homogeneous neutrons strong in intensity relative to that of the immediately neighboring energy regions is present. Though there is not a sufficient number of tracks in this survey for good statistics, the intensity between 11 Mev and 12 Mev appears less than 20 percent of that between 12 Mev and 13 Mev. The width of the group appears to be over 1.25 Mev, as compared with a calculated maximum of 0.85 Mev. Multiple small angle scattering in the collimator, pressure variation in the cloud chamber, and errors in measurement probably account for this additional spread.

The average yield of tracks per picture was increased to more than one high energy track every two pictures by applying the cyclotron arc voltage at the beginning of the expansion and increasing the stability of the cyclotron arc operation. This was effective since the chamber

[12] E. C. Pollard and W. L. Davidson, *Applied Nuclear Physics* (John Wiley and Sons, Inc., 1942), Appendix 7.

was now exposed a longer time to the incident neutrons, and even when the arc delayed in firing, it was more likely to produce some deuterons sufficiently early for use. The compressed chamber gauge pressure was set at 335 pounds per square inch. The scattering data were taken in 36 runs, each "run" consisting of continuous operation of the chamber for approximately three hours between changing of rolls of film in the camera. The tracks were measured with the apparatus and procedure already described. As before, only those proton tracks which were distinct, fully in the light beam, wholly inside the chamber, and which originated in the path of the neutron beam across a diameter of the chamber, were considered as valid for data. Most of the tracks appeared uniformly dense along their lengths, with a slight increase in density near their terminal end. The maximum and minimum proton ranges that could correspond to a 12.0 Mev to 13.0 Mev neutron were known from a calculation to be described, and

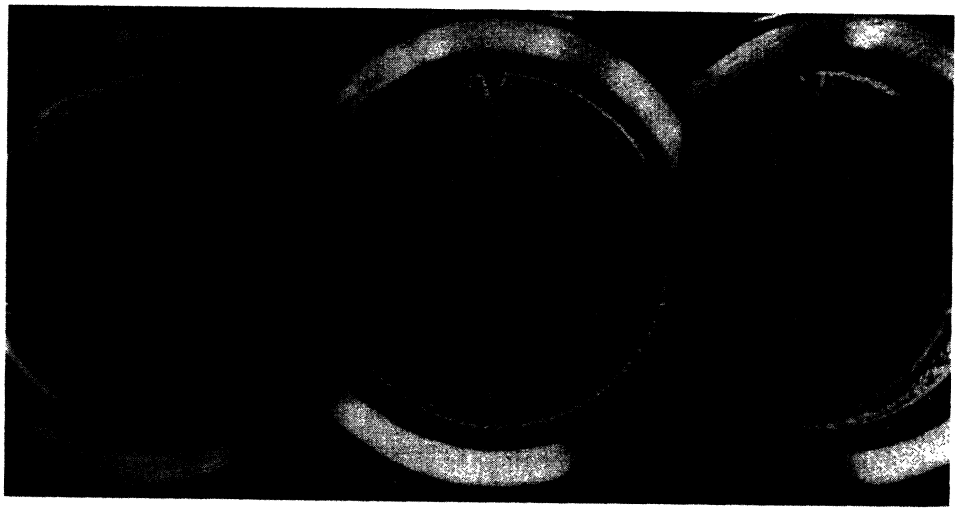

FIG. 4. Recoil protons in the high pressure cloud chamber. The expansion ratio was adjusted to minimize density of the electron tracks.

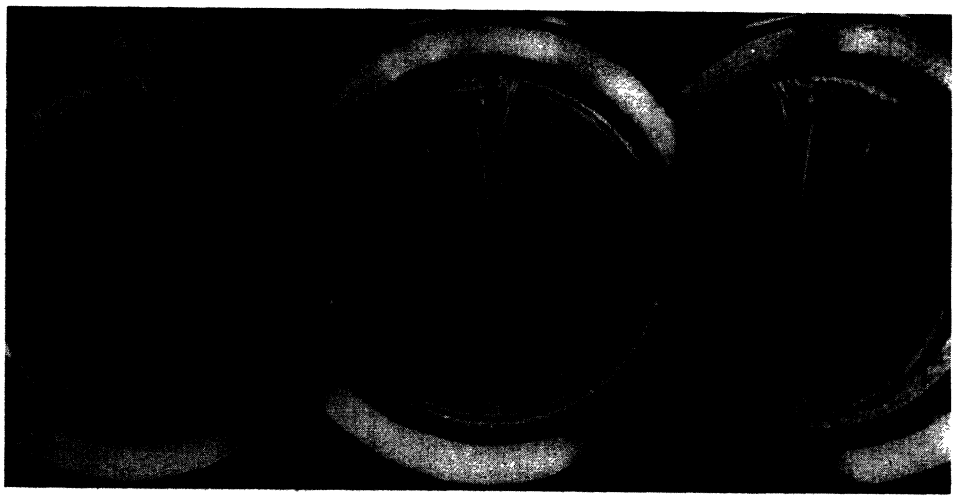

FIG. 5. Recoil protons in the high pressure cloud chamber. The effect of collimation is evident. The less dense tracks are electron tracks.

TABLE I. Cloud chamber stopping power.

Recoil angle interval, degrees	Stopping power Max. pressure	Min. pressure
0–10	19.35	17.30
11–20	19.36	17.31
21–30	19.42	17.40
31–40	19.55	17.50
41–50	19.75	17.65

particular care was exercised to measure all tracks that could possibly fall within this region. Energetically the examined region extended from below 10.5 Mev to above 14.5 Mev, with certainty that no tracks in the pertinent region were missed. Figures 4 and 5 show some pictures of the proton tracks. These pictures show more than one proton track and thus show the effect of collimation of the neutrons. Over 1900 tracks were measured.

Five cases of 3-prong tracks were recorded on the photographs. Energy and momentum conservation considerations required that all of the prongs be proton tracks. These were, therefore, instances in which neutron-proton scattering was followed by proton-proton scattering.

Using the maximum and minimum pressures in the chamber and the stopping power of the gas, the maximum and minimum lengths of the protons recoiled from collisions with neutrons of energy between 12.0 Mev and 13.0 Mev were calculated as a function of recoil angle. The maximum and minimum gauge pressures were 335 pounds per square inch and 298 pounds per square inch, respectively, which correspond to absolute pressures of 23.8 atmospheres and 21.3 atmospheres. For each recoil angle in one-degree intervals the energy of the proton recoils corresponding to 12.0 Mev and 13.0 Mev neutrons and their ranges in air were calculated from the relation $E_p = E_n \cos^2\phi$ and from the range-energy curve. Before this length in air was converted into the track length in the chamber, the variation of the stopping power of methane with proton energy was evaluated from the curves given by Bethe.[18] This variation was small and is more important from the standpoint of consistency rather than accuracy. The median proton energy corresponding to the median recoil angle in each 10° recoil angle interval was taken as the average proton energy for each of these intervals. The length in air corresponding to these proton energies was obtained and the stopping power of methane determined for each length. The chamber stopping power as a function of recoil angle in 10° intervals for maximum and minimum pressure is given in Table I. These maximum and minimum stopping powers, together with the lengths of the recoil proton tracks determined for each recoil angle, yielded the maximum and minimum ranges of a proton projected by a neutron with energy between 12.0 Mev and 13.0 Mev as a function of recoil angle ϕ. These ranges are given in Table II.

The tracks in the data which fell within the range limits corresponding to their measured recoil angle ϕ were tabulated simultaneously in 5° recoil angle intervals and 10° azimuthal angle intervals. This tabulation was also repeated for those tracks which either fell within the range limits corresponding to their measured recoil angle ϕ or also those of the neighboring recoil angles $\phi \pm 1°$. This tabulation was also repeated for larger recoil angle intervals. Though the error in measurement of the recoil angle was as much as $\pm 2°$, since the neutron spectrum was peaked between the 12.0 Mev and 13.0 Mev limits used, the overlapping of the range limits for neighboring recoil angles was apparently

TABLE II. Maximum and minimum proton track length allowed for each recoil angle.

Recoil angle degrees	Track length limits cm	Recoil angle degrees	Track length limits cm	Recoil angle degrees	Track length limits cm
0	8.20–10.55	21	6.35–8.3	41	3.0 –3.9
1	8.2 –10.5	22	6.2 –8.0	42	2.8 –3.6
2	8.1 –10.5	23	6.1 –7.8	43	2.7 –3.4
3	8.1 –10.5	24	5.9 –7.6	44	2.5 –3.2
4	8.00–10.40	25	5.8 –7.4	45	2.4 –3.0
5	8.00–10.4	26	5.6 –7.2	46	2.3 –2.9
6	8.0 –10.4	27	5.4 –7.0	47	2.1 –2.7
7	7.9 –10.3	28	5.3 –6.8	48	2.0 –2.5
8	7.9 –10.3	29	5.1 –6.6	49	1.8 –2.4
9	7.8 –10.15	30	4.9 –6.3	50	1.7 –2.2
10	7.7 –10.0	31	4.7 –6.0	51	1.6 –2.0
11	7.65– 9.9	32	4.5 –5.8	52	1.5 –1.9
12	7.54– 9.75	33	4.3 –5.6	53	1.4 –1.7
13	7.44– 9.6	34	4.15–5.4	54	1.3 –1.6
14	7.28– 9.5	35	4.0 –5.1	55	1.2 –1.5
15	7.19– 9.3	36	3.8 –4.9	56	1.1 –1.4
16	7.08– 9.2	37	3.7 –4.7	57	0.97–1.25
17	6.98– 9.0	38	3.5 –4.5	58	0.87–1.14
18	6.88– 8.9	39	3.3 –4.3	59	0.77–1.0
19	6.67– 8.7	40	3.1 –4.1	60	0.66–0.90
20	6.55– 8.5				

[18] H. A. Bethe, Rev. Mod. Phys. 9, 275 (1937).

sufficient to include most of the tracks whose measured recoil angle had an error of $\pm 2°$. As a consequence, the $\phi \pm 0°$ and $\phi \pm 1°$ scattering angle tabulations differed by small percentages. The 1573 tracks selected with the $\phi \pm 0°$ recoil angle selection criterion are used in this analysis, though essentially similar results are obtained on the basis of the 1636 tracks selected with the less rigorous $\phi \pm 1°$ recoil angle selection criterion. An analysis based on the tracks selected with the less rigorous $\phi \pm 1°$ recoil angle selection criterion was reported earlier.[14]

The total number of tracks measured in 10° recoil angle intervals has been plotted against their ranges in the chamber. These plots are shown in Fig. 6. The total number is the sum of the solid and dashed plots, where the solid lines represent the tracks which fell within the calculated ranges for the measured recoil angle. These are not spectrum plots, since tracks of the same length could correspond to different neutron energies. This is because, as shown in Table II, tracks of different lengths corresponding to the same recoil angle were acceptable. Since the proton energy varies as the squares of the cosine of the scattering angle ϕ, the change in proton energy for a given change in recoil angle will increase as the angle ϕ increases. Also a given change in length will be relatively more important energy-wise at the lower proton energies (larger recoil angle ϕ) since their ranges are shorter. For these reasons, the overlapping of different energies into a single range will increase as the recoil angle increases. However, at the smaller recoil angles the different energies will be more spread apart and the range plot will bear more of a resemblance to a spectrum plot. The plot for the recoil angle interval 0°–10° would therefore represent the spectrum within statistical limitations.

As described above, the experimental data were tabulated according to their azimuthal distribution. Since the neutron-proton scattering process is azimuthally symmetrical, the number in each azimuthal angle interval should be constant if all the tracks were fully within the illuminated region of the cloud chamber. The following factors influence the actual azimuthal distribution:

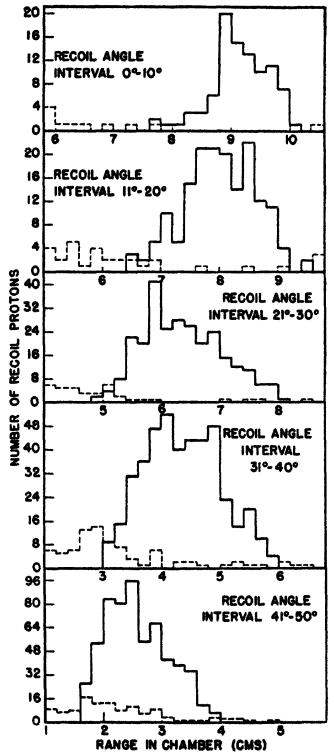

FIG. 6. Number of recoil protons *vs.* range in the high pressure cloud chamber. The solid plot indicates the number of recoil protons selected by use of the $\phi \pm 0°$ recoil angle selection criterion. The dashed plot shows some of the recoil protons excluded by this criterion. The recoil angle intervals are in the laboratory system.

(a) the finite height of the volume illuminated by the parallel light beam,
(b) the finite diameter of the neutron beam,
(c) the spread of lengths in each recoil angular interval.

The expected azimuthal distribution can be calculated on the basis of purely geometrical considerations. In Fig. 7, $2d$ represents the height of the light beam, while r represents the projection of a recoil in a plane normal to the neutron beam. The quantity r is given numerically by the relation $r = L \sin\phi$. θ' is the largest azimuthal angle at which r is still included in the light beam. Because of the finite size of the neutron beam, a track that starts above center will have less chance of being seen in the upper half but more chance of being seen in the lower half. For such a track the value of θ' above center (θ_a') will be smaller, while the corre-

[14] J. S. Laughlin and P. G. Kruger, Phys. Rev. **71**, 736 (1947).

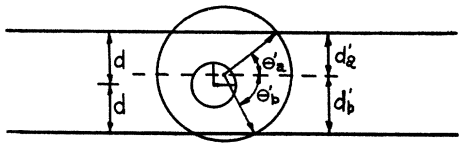

FIG. 7. Geometrical relation between the neutron beam and the illuminated chamber volume.

sponding value of θ' below center (θ_b') will be larger, than if it started at the center. The distribution of neutrons can be considered uniform in the one-half inch diameter circle, so the probability P of the track being illuminated will be determined for one quadrant. If y represents the vertical distance from the center at which the track originates, the remaining distance to the upper and lower edges of the light beam will be $d_a'=d-y$ and $d_b'=d+y$, respectively. The maximum value of y will be $b=\frac{1}{4}$ inch. The expression for P now becomes:

$$P=\left[\int_0^b\int_0^{(b^2-y^2)^{\frac{1}{2}}}\frac{2}{\pi}\sin^{-1}\frac{d-y}{r}dxdy+\int_0^b\int_0^{(b^2-y^2)^{\frac{1}{2}}}\frac{2}{\pi}\sin^{-1}\frac{d+y}{r}dxdy\right]\frac{1}{dxdy}.$$

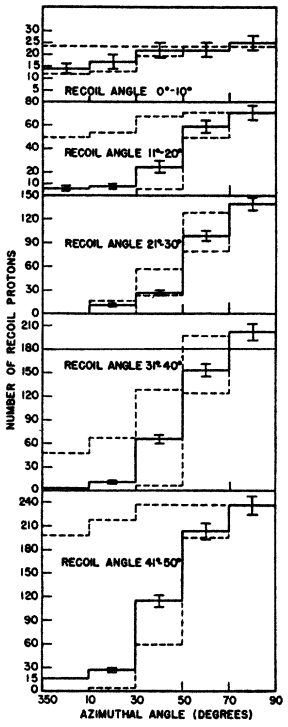

FIG. 8. Azimuthal distribution of the recoil protons. The dashed plots indicate the calculated maximum and minimum limits for the number of recoil protons which could have been observed under the limitation of the cloud chamber geometry relative to the observed number plotted in the solid graph. The number of recoil protons plotted in a given azimuthal angle interval includes all those in the corresponding azimuthal angular interval in all four quadrants of the azimuthal plot. For instance, the number plotted in the azimuthal interval 70° to 90° includes those observed in the intervals 70° to 90°, 90° to 110°, 250° to 270°, and 270° to 290°.

The quadrant was divided into ten segments and the expression for P integrated numerically. For each 10° recoil angle interval, this calculation has been carried out for the maximum and minimum values of r that occur in that interval. The azimuthal distributions obtained from these values of r should be the extremes, and the experimental azimuthal distribution would be expected to fall between these extremes. The azimuthal distribution was considered in 20° azimuthal angle intervals. Each azimuthal angular interval was weighted according to the probability of a track originating from each quadrant segment being seen in that azimuthal interval, this weight in turn being weighted by the fractional area of the quadrant belonging to that particular segment. These weights were then determined in each 20° azimuthal interval for each segment and added, yielding the relative probability of a track being illuminated in each 20° azimuthal interval. Figure 8 shows the plotted results. The dashed lines represent the calculated extreme azimuthal angle distributions, while the solid line is the experimental distribution. Probable errors, a measure of statistical uncertainty ($0.6745(n)^{\frac{1}{2}}$) are indicated. The data have been "folded over" azimuthally for the experimental plots so that all of the data are represented in the one azimuthal quadrant indicated, e.g., in Fig. 9 in the 0° to 10° recoil angle interval 25 tracks are plotted in the 70° to 90° azimuthal angle interval. This includes tracks from the 70° to 109° and 250° to 289° azimuthal angular intervals.

The coincidence of the dashed lines for certain end intervals indicates that all the tracks should have been seen in those azimuthal intervals. Accordingly, the experimental data were normalized to coincide for those intervals. If all the data occurring in the various azimuthal intervals are to be used, an azimuthal correction factor

TABLE III. Experimental data for angular distribution of recoil protons with azimuthal correction factor of unity.

Recoil angle interval in center-of-mass system	Total no. of recoil protons	No. of recoil protons in fully illuminated azimuthal intervals	Length correction factors	Corrected no. of recoil protons	Solid angle of indicated recoil and azimuthal angle intervals	Corrected no. of recoil protons per unit solid angle	Relative no. of recoil protons per unit solid angle
0– 21	93	47*	2.78	131	0.1845	708	1.21±0.12
21– 41	166	71	2.31	164	0.250	656	1.12±0.09
41– 61	277	140	1.84	258	0.378	682	1.17±0.06
61– 81	435	203	1.41	286	0.459	623	1.07±0.05
81–101	593	238	1.19	284	0.485	584	1.00±0.04

* No. of recoil protons in those azimuthal intervals corresponding to 50° to 90°.

would be necessary. However, if the light beam had been sufficiently deep, all tracks would have been illuminated over their full length in all the azimuthal intervals and thus would have been measured. In this case, both the calculated extremes would have been horizontal lines. Therefore, the area under a horizontal line extended across from the end interval represents the number of tracks that would have been seen if no correction were necessary. An azimuthal correction factor would be unnecessary if only those data were used which fell in those azimuthal angular intervals in which all the tracks were fully illuminated. In the final analysis in Table III only these data appearing in these particular end azimuthal zones are employed, and the azimuthal correction factors are consequently unity and do not appear.

The actual experimental azimuthal distribution would be expected to fall between the calculated extreme azimuthal distributions. If the assumptions could be made that the spectrum of the high energy neutron group was completely symmetrical, that the neutrons entered the chamber in uniform numbers throughout the expansion, and that the different track lengths above and below the median track lengths in each recoil angle interval were equally probable, the experimental distribution would be expected to be halfway between the calculated extremes. Though these simplifying assumptions are not necessarily valid, for the purpose of comparison with the results in Table III, the calculated extreme azimuthal distributions are represented in Table IV by correction factors based on the median of the calculated azimuthal distributions. The calculated azimuthal correction factor is the ratio of the area under the horizontal line extended across from the end interval at 90° to 0° to the area under the median of the calculated distribution between azimuthal angles 0° and 90°. An examination of the plots shows that the experimental azimuthal distribution falls within the calculated extremes in a reasonable manner. In the azimuthal angular interval from 0° to 30° in the plot for the 41° to 50° recoil angle interval the experimental points are markedly low. Although great care was taken to measure all pertinent tracks, the most plausible explanation for the low values of these particular experimental points is that some tracks were missed. In the azimuthal positions of the viewing screen in which most of the tracks occurred and were measured, the tracks in this particular azimuthal and recoil angular interval would have the shortest projections of any of the tracks ex-

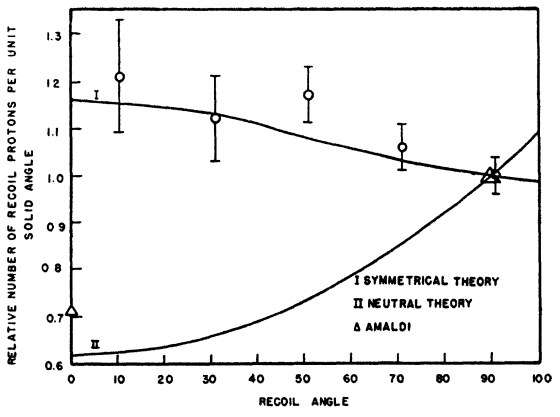

FIG. 9. Relative number of recoil protons per unit solid angle in center-of-mass system normalized to unity at the 90° recoil angle. This indicates a ratio of unity or somewhat greater than unity for backward scattering of neutrons to that at right angles with respect to the incident neutron beam. The angular distributions predicted by a symmetrical type of theory and a neutral type of theory are plotted. A comparison is also made with some of Amaldi's experimental results.

TABLE IV. Experimental data for angular distribution of recoil protons with calculated azimuthal correction factor.

Recoil angle interval in center-of-mass system	Number of recoil protons	Calculated azimuthal correction factor	Length correction factor	Corrected no. of recoil protons	Solid angle of indicated recoil and azimuthal angle interval	Corrected no. of recoil protons per unit solid angle	Relative no. recoil of protons per unit solid angle
0– 21	93	1.12	2.78	290	0.415	698	1.25±0.09
21– 41	166	1.81	2.31	692	1.125	615	1.10±0.06
41– 61	277	2.19	1.84	1115	1.698	658	1.18±0.05
61– 81	435	2.10	1.41	1287	2.083	617	1.11±0.04
81–101	557*	1.22	1.19	810	1.452	557	1.00±0.03

* Does not include recoils in azimuthal angle intervals corresponding to 0° to 30°.

amined. For this reason, the calculated azimuthal correction factor in Table IV for the 81°–101° recoil angle interval (center of mass system) is based on the azimuthal region 30° to 90° and on the corresponding regions in the other three azimuthal quadrants, i.e., 90° to 150°; 210° to 270°; and 270° to 330°.

A length correction factor is necessary since the track length is different for each different recoil angle. The recoil protons have a uniform probability of originating at any point in the neutron beam which is along a diameter of the chamber, However, the distance along this path in which the track can originate and end within the chamber will increase with decreasing track length and increasing recoil angle. The ratio of the diameter of the cloud chamber to that portion of the diameter in which the track can originate and be entirely within the chamber is the length correction factor. The average length of track in each recoil angle interval was calculated, and the ratio then geometrically determined. The length correction factors are listed in Tables III and IV.

The analysis of the data is given in Table III. The first column lists the recoil angle intervals in the center-of-mass system into which the data have been analyzed. The second column gives the total number of proton recoils which satisfied the $\phi\pm0°$ recoil angle selection criterion. The third column gives the number of recoil protons in those azimuthal angle intervals which were fully illuminated. Unless otherwise noted, these azimuthal intervals were those corresponding to the 70° to 90° interval in the first azimuthal quadrant. The fourth column gives the length correction factors. The fifth column contains the number of recoils after application of the length correction factor. The sixth column gives the solid angle corresponding to the indicated recoil and azimuthal angular intervals. The seventh column gives the number of corrected tracks per unit solid angle. The last column gives the ratio of the number of recoil protons per unit solid angle in the center-of-mass system in the indicated recoil angle interval to the number in the 81° to 101° recoil angle interval. Probable errors, based on the number of tracks in the third column, are also indicated.

In Table IV is an analysis on the basis of the calculated azimuthal correction factors. The second column gives the total number of tracks in the indicated recoil angle intervals. The number of tracks in the 81°–101° interval does not include those between azimuthal angles corresponding to 0° and 30°. The third column contains the calculated azimuthal correction factors based on a median of the calculated extreme distributions. The fourth column contains the length correction factors, and the fifth the corrected number of recoil tracks. The sixth shows the solid angle corresponding to the indicated recoil and azimuthal angle interval. The seventh column shows the corrected number of recoils per unit solid angle. The last column gives the ratios defined above. The general trend of the ratios in Table IV is in agreement with that of Table III. The analysis in Table III is considered more reliable since the azimuthal correction factors have been eliminated.

In Fig. 9 the experimental data of Table III are compared with two theoretical curves. A form of the "symmetrical" theory yields the expression as given by Rarita, Schwinger, and Nye.[15]

[15] William Rarita, Julian Schwinger, and H. A. Nye, Phys. Rev. 59, 209 (1941).

$$\sigma \sim (1-0.080\cos\phi+0.077\cos^2\phi)$$

for the distribution in the center-of-mass system. This distribution is denoted by I in Fig. 9. The "cut-off neutral theory of Bethe[16] as calculated by Kittel and Breit[17] for 16 Mev neutrons gave the expression:

$$\sigma \sim (1+0.46\cos\phi+0.094\cos^2\phi).$$

This distribution is plotted as II in Fig. 9.

[16] H. A. Bethe, Phys. Rev. 57, 390 (1940).
[17] C. Kittel and G. Breit, Phys. Rev. 56, 744 (1939).

With regard for the statistical limitations present in these data, it appears that a ratio of the differential cross sections for the scattering of neutrons in the backward direction to the scattering of neutrons in the direction perpendicular to that of the incident neutron beam equal to unity (spherically symmetric scattering), or slightly greater than unity can be consistent with these data. This result favors meson nuclear force theories of the "symmetrical" type and is in disagreement with "neutral" theories or any theory involving ordinary forces only.

PHYSICAL REVIEW VOLUME 73, NUMBER 3 FEBRUARY 1, 1948

Range-Energy Relations for Protons in Substances Containing C, H, O, A, and Xe*,**

J. O. HIRSCHFELDER† AND J. L. MAGEE‡
Los Alamos Scientific Laboratory, Los Alamos, New Mexico

(Received October 6, 1947)

The Bethe theory was used to calculate the stopping power of protons in C, H, O, A, and Xe. The range-energy curves for protons in glycerol tristearate ($C_{57}H_{110}O_6$), paraffin ($(CH_2)_n$), argon, and xenon are presented. The calculations for C, H, and paraffin are carried to 15 Mev, whereas all the others are only given up to 3 Mev.

BETHE'S[1] method can be used to determine the range-energy relations for fast protons passing through various substances. The functional form of the equations is valid provided that the energy is larger than around 0.1 Mev. Actually we have used these equations down to energies of 0.005 Mev in order to calculate the absolute value of the range (even rather large errors in the stopping power over this energy interval do not appreciably effect the value of the range for high energy protons). The method is semi-empirical in the sense that the effective ionization potential for the electrons in the outermost shell is adjusted to fit an experimental value of an alpha particle range. The other constants in the equations are chosen *a priori* from theoretical considerations.

I. THEORETICAL EQUATIONS

The change of energy, E(Mev), with residual range, R(cm), for protons is given by:

$$dE/dR=2\pi e^4(M/m)N(B/E). \quad (1)$$

Here, $M/m=1836.6$, which is the ratio of mass of proton to mass of electron; e is the electronic charge (for our purposes it is convenient to take $e^2=14.397\times10^{-8}$ electron volt cm); and N is the number of atoms per cc. The dimensionless quantity B is called the stopping number. For a gas under standard conditions, Eq. (1) becomes:

$$dE/dR=0.006094B/E. \quad (2)$$

The stopping number is closely related to the atomic stopping cross section (electron volt cm²):

$$\sigma\times10^{15}=0.2392B/E, \quad (3)$$

* This paper is a revision of part of the material contained in the declassified Los Alamos Report LADC-124.

** This document is based on work performed at Los Alamos Scientific Laboratory of the University of California under Government Contract W-7405-eng-36 and the information contained therein will appear in Division V of the National Nuclear Energy Series (Manhattan Project Technical Section) as part of the contribution of the Los Alamos Laboratory.

† Now in the Department of Chemistry, University of Wisconsin.
‡ Now at Argonne National Laboratory.

[1] H. Bethe, *Handbuch der Physik* Vol. 24 Part I, p. 521; M. Livingston and H. Bethe, Rev. Mod. Phys. 9, 263 (1937); J. Ashkin, H. Bethe, and V. Weisskopf, LADC-116 (1943); N. F. Mott and H. S. W. Massey, *The Theory of Atomic Collisions* (Oxford University Press, 1933), p. 224.

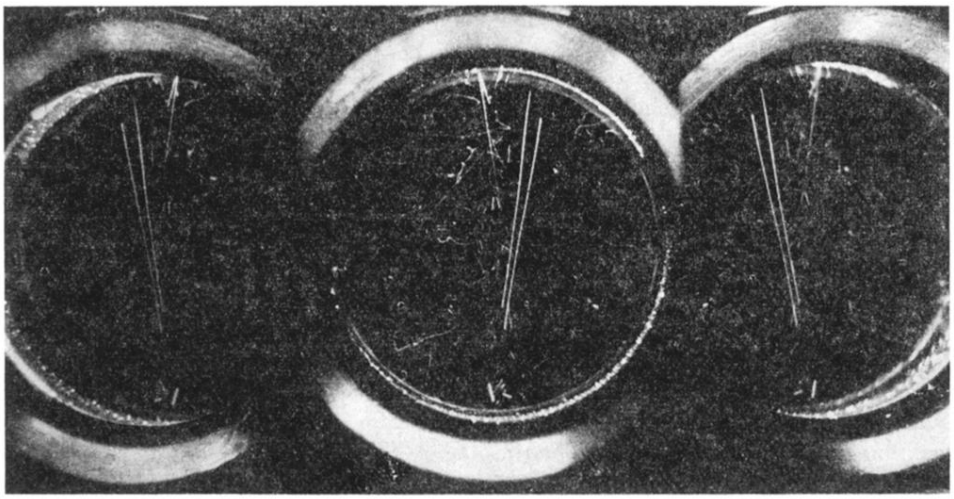

FIG. 4. Recoil protons in the high pressure cloud chamber. The expansion ratio was adjusted to minimize density of the electron tracks.

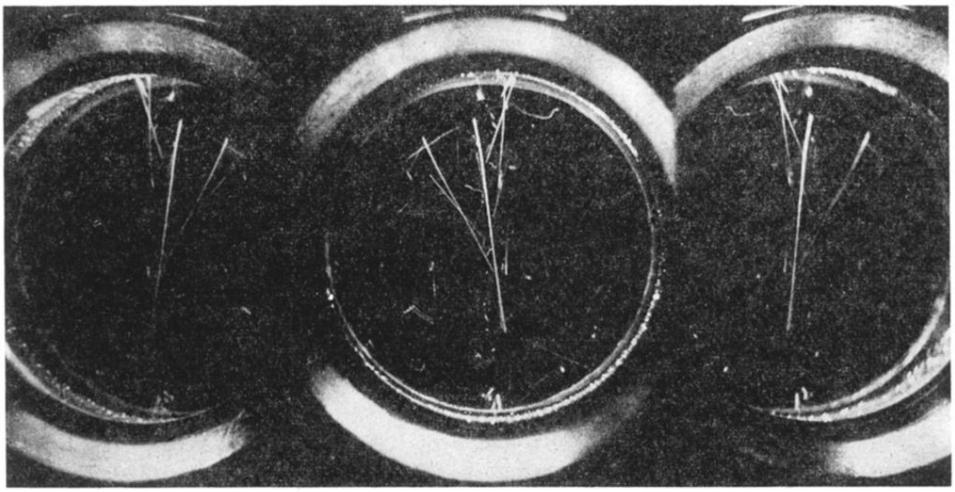

FIG. 5. Recoil protons in the high pressure cloud chamber. The effect of collimation is evident. The less dense tracks are electron tracks.